Journal of Clinical Laboratory Analysis

WILEY

CASE REPORT OPEN ACCESS

Novel Germline *KIT* Variants in Families With Severe Piebaldism: Case Series and Literature Review

Yuanyuan Zhang[1] | Haiming Gao[1] | Lu Zhang[1] | Yunjing Zhao[2] | Chuang Qiu[3] | Xiaoliang Liu[1]

[1]Department of Clinical Genetics, Shengjing Hospital of China Medical University, Shenyang, China | [2]Department of Developmental Pediatrics, Shengjing Hospital of China Medical University, Shenyang, China | [3]Department of Orthopedics, Shengjing Hospital of China Medical University, Shenyang, China

Correspondence: Chuang Qiu (qiuc@sj-hospital.org) | Xiaoliang Liu (liuxl@sj-hospital.org)

Received: 16 November 2023 | **Revised:** 15 May 2024 | **Accepted:** 17 May 2024

Funding: This study was supported by General Project of Shengjing Hospital (M1116 and M1643), 345 Talents of Shengjing Hospital (M1395), National Natural Science Foundation of China (32300488), and Natural Science Foundation of Liaoning Province (2022-MS-208).

Keywords: depigmentation | gene variant | *KIT* | piebaldism

ABSTRACT

Introduction: Piebaldism is a rare autosomal dominant disorder characterized by congenital white forelock and depigmented patches, which is most commonly caused by deleterious variants in the *KIT* gene.

Methods: Four *KIT* variants were identified in a piebaldism case series by whole-exome sequencing. Functional experiments, including in vitro minigene reporter assay and enzyme-linked immunosorbent assay, were carried out to elucidate the pathogenicity of the variants. The genotype–phenotype correlation was summarized through extensive literature reviewing.

Results: All the four cases had severe piebaldism presented with typical white forelock and diffuse depigmentation on the ventral trunk and limbs. Four germline variants at the tyrosine kinase (TK) domains of the *KIT* gene were identified: two novel variants c.1990+1G>A (p.Pro627_Gly664delinsArg) and c.2716T>C (p.Cys906Arg), and two known variants c.1879+1G>A (p.Gly592_Pro627delinsAla) and c.1747G>A (p.Glu583Lys). Both splicing variants caused exon skipping and inframe deletions in the TK1 domain. The missense variants resided at the TK1 and TK2 domains respectively impairing PI3K/AKT and MAPK/ERK signaling pathways, the downstream of KIT. All severe cases were associated with variants in the TK domains, eliciting a major dominant-negative mechanism of the disease.

Conclusion: Our data expand the mutation spectrum of *KIT*, emphasized by a dominant-negative effect of variants in the critical TK domains in severe cases. We also share the experience of prenatal diagnosis and informed reproductive choices for the affected families.

1 | Introduction

Piebaldism (MIM 172800) is an autosomal dominant pigment disorder characterized by congenital depigmented patches on the central frontal scalp, central forehead, ventral trunk, and extremities [1]. The disease is rare with an estimated prevalence of <1:20,000 individuals, without gender bias [2]. White patches are present at birth and stay commonly stable throughout life, whereas sometimes hyperpigmented macules (café-au-lait macules) can develop at the margins or within depigmented patches. Phenotypic severity is classified according to the range of depigmented patches. Mild cases have white forelock only or small guttate leukoderma only in the ventral trunk and limbs. Severe cases have typical white forelock and large white spots on the chest, abdomen, and limbs. And moderate cases have intermediate degrees [1]. Other presentations,

Yuanyuan Zhang and Haiming Gao contributed equally to this work.

including deafness, heterochromia irides, and brown hair, have been rarely observed [3, 4].

Piebaldism is most commonly caused by germline variants in the *KIT* gene (MIM 164920) localized on chromosome 4q12 [5]. As a member of the type III transmembrane receptor tyrosine kinase (TK) family, the KIT protein is structurally composed of a signal sequence (SS, 1–22 aa), an extracellular ligand-binding domain (EC, 23–520 aa), a transmembrane domain (TM, 521–543 aa), a juxtamembrane domain (JM, 544–581 aa), and a split TK domain with two lobes (TK1, 582–684 aa; TK2, 762–937 aa) linked by a kinase insert domain (KI, 685–761 aa) [6]. The KIT homodimerizes after binding to its ligand, stem cell factor (SCF), and activates subsequent signal transduction, such as the PI3K/Akt and MAPK cascades [7, 8]. Variants in *KIT* disrupt melanocyte development and migration from the neural crest and cause the absence of melanocytes in the ventral midline of the epidermis [9]. Variant types at various structural domains correlate with divergent clinical features and severity of piebaldism [10], and patients in the same family may have different phenotypes [11]. Additionally, mutations in the *SNAI2* gene (MIM 602150) on chromosome 8q11.21, a zinc-finger neural crest transcription factor for maintaining melanoblast homeostasis, have also been implicated in cases with piebaldism [12].

Herein, we report four cases with severe piebaldism caused by germline *KIT* variants at TK domains, including two novel variants. The potential molecular mechanisms of the variants were elucidated. All cases of *KIT*-related piebaldism have been reviewed in literature to characterize a genotype–phenotype correlation.

2 | Materials and Methods

2.1 | Cases Selection and Clinical Evaluation

Four cases with pigment disorders were outpatients enrolled from Shengjing Hospital of China Medical University. They are of Han ethnicity from Northeast China. Extensive physical examination was performed to evaluate the distribution, shapes, and areas of the depigmented patches as well as café au lait lesions. The disease progression and familial histories were also carefully recorded. Ophthalmic, auditory, and brain MRI examination as well as blood routine tests were performed in the young Proband 2 to exclude extracutaneous involvement. Pathological examination was not performed considering the invasive skin biopsy. The study was conducted in accordance with the Helsinki Declaration of 1964 and its later amendments and approved by the Ethics Committee of Shengjing Hospital of China Medical University (2021PS523K).

2.2 | Genetic Analysis

Mutation analysis was performed after obtaining written informed consents of the four probands and their family members. Peripheral blood samples were collected and genomic DNA (gDNA) was isolated using QIAamp DNA Blood Mini Kit (QIAGEN, Germany) according to the manufacturer's instructions. Whole-exome sequencing (WES) was performed to screen for pathogenic variants. The genes were enriched using biotinylated capture probes (MyGenostics, Baltimore, MD, USA) as described previously [13] and were sequenced on the Illumina-Hiseq4000 platform (San Diego, CA, USA) with 50× coverage. Variant calling was performed using NCBI37/hg19 assembly of human genome as reference sequences. The candidate causative variants were furthermore confirmed by Sanger sequencing in all the family members. Target DNA fragments encompassing the variants were amplified using the Superstar HiFi DNA Polymerase (GeneStar Bio, Qingdao, China). Sanger sequencing was performed using the BigDye Terminator v3.1 Cycle Sequencing Kit (Applied Biosystems, Carlsbad, CA, USA) on an ABI Prism 3730 Genetic Analyzer (Applied Biosystems).

2.3 | Minigene Reporter Assay

Splicing destruction was further analyzed using an in vitro minigene reporter assay. Wild-type and the corresponding mutant amplicons of the *KIT* gene (NM_000222.3) were obtained from the gDNA of normal control, Proband 1, and Proband 2, using the following primers F: 5′-ggatccGACATCAGTTTGCC-3′; R: 5′-gctagcATTATTGGAAGACATG-3′ for the c.1990+1G>A variant and F: 5′-ggatccAGTATGAAACAGGGGCTTTCC-3′; R: 5′-gctagcGCAAACTGATGTCAAGCGC-3′ for the c.1879+1G>A variant. The primers were added with restriction enzyme cutting sites of *Bam*HI and *Nhe*I to the 5′-terminus. PCR products were cloned into the pSPL3 vector that was kindly provided by Professor Leping Shao (The Affiliated Qingdao Municipal Hospital of Qingdao University, China). The wild-type and mutant constructs were verified by Sanger sequencing and then transfected into human embryo kidney (HEK293T) cells using jetPEIDNA transfection Reagent (Polyplus, France) according to the manufacturer's instruction. After 24h of transfection, RNA was extracted using TransZol Up Plus RNA Kit (TransGen Biotech, Beijing, China), and cDNA was synthesized using PrimeScript RT reagent Kit with gDNA Eraser (Takara, Dalian, China) according to the manufacturer's instructions. The cDNA products were used as templates for PCR amplification with the following pSPL3 vector-specific primers 5′-TCTGAGTCACCTGGACAACC-3′ and 5′-ATCTCAGTGGTATTTGTGAGC-3′ for *KIT*, as well as 5′-CCTGGCACCCAGCACAAT-3′ and 5′-GGGCCGGACTCGTCATAC-3′ for β-actin as internal control. The splicing transcripts were analyzed by electrophoresis on a 2% agarose gel and verified by Sanger sequencing.

2.4 | In Silico Analysis

In silico tools including PolyPhen2 (http://genetics.bwh.harvard.edu/pph2), REVEL (https://sites.google.com/site/revelgenomics), SIFT (http://sift.jcvi.org), MutationTaster (https://www.mutationtaster.org/), and M-CAP (http://bejerano.stanford.edu/mcap/) were used to analyze the pathogenicity of the missense variants. ESEfinder (http://krainer01.cshl.edu/cgi-bin/tools/ESE3/esefinder.cgi?process=home), FSplice (http://www.softberry.com/berry.phtml?topic=fsplice&group=programs&subgroup=gfind), NNSplice (http://www.fruitfly.org/seq_tools/splice.html), and NetGene2 (http://www.cbs.dtu.dk/services/NetGene2) tools were applied to predict splicing changes. The evaluation of the KIT amino acid conservation was performed by the Ugene software. The three-dimensional (3D) molecular

model was built using AlphaFold (https://www.alphafold.ebi.ac.uk/), and structural change was visualized using the PyMOL software (https://pymol.org/2/).

2.5 | Enzyme-Linked Immunosorbent Assay (ELISA)

The human wild-type, Cys906Arg and Glu583Lys mutant KIT expression vectors were synthesized by GeneChem Co., Ltd. (Shanghai, China). HEK293T cells were transfected with wild-type or mutant plasmids for 24 h and then treated with 100 ng/mL SCF for 2 h. Total protein was extracted from cell lysate and the phosphorylated AKT (p-AKT) and ERK (p-ERK) was determined using the human p-AKT ELISA kit (Bioswamp, Wuhan, China) and human p-ERK ELISA Kit (Elabscience, Wuhan, China) according to the instructions. The absorbance value was measured spectrophotometrically at wavelength of 450 nm. The results were expressed by relative concentrations. The entire assay was performed in triplicate.

3 | Results

3.1 | Case Presentation

Proband 1 was a 34-year-old man who wanted genetic diagnosis of his depigmentation. He had a white patch in the middle forehead (forelock dyed in the photo), partial poliosis of eyebrows, and extensive areas of depigmentation on the abdomen and limbs with white body hair, and islands of hyperpigmented café-au-lait macules in the affected areas. A large four generations pedigree is drawn including 10 affected individuals presented with similar leukoderma (Figure 1a).

Proband 2 was a 7-year-old boy who was referred to Developmental Pediatrics for attention deficit and learning problems. He had piebaldism features including typical white forelock, V-shaped hypopigmented patch on the forehead, and large range of leukoderma with pigmented spots on the abdomen and limbs. Ophthalmic, auditory, and brain MRI examination as well as blood routine tests all returned with normal results. The

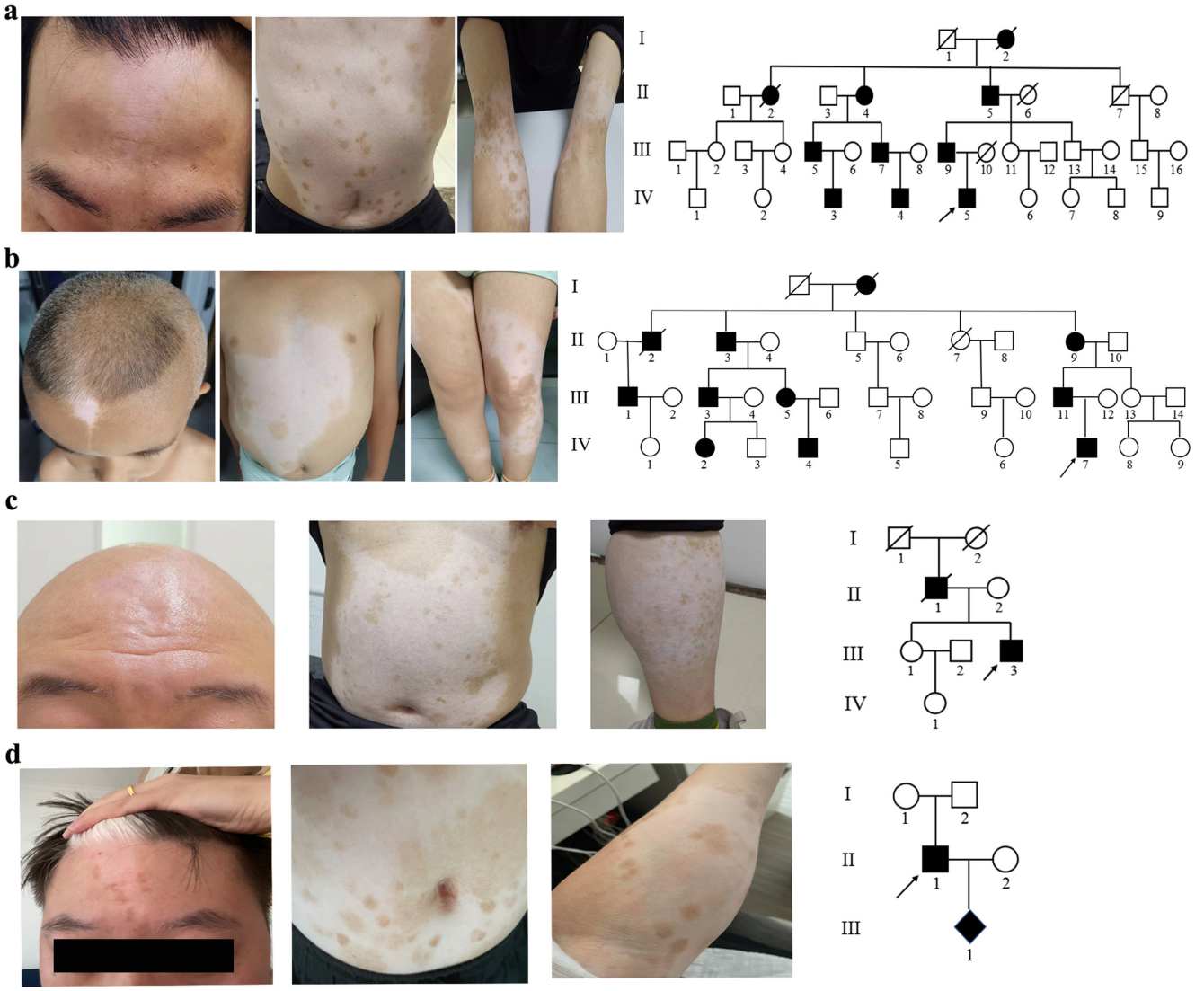

FIGURE 1 | Photographs and family pedigrees of four cases with piebaldism. All the four probands had a typical severe presentation, including white forelocks, V-shaped hypopigmented patches on the forehead, and large ranges of leukoderma with pigmented spots on the abdomen and limbs (a, b, c and d). Partial poliosis of eyebrows and body hairs could be observed in Proband 3 (c). The family pedigrees indicate an autosomal dominant inheritance pattern. *Note*: Proband 1 (a) had dyed his hair.

leukoderma was inherited from his similarly affected father. An unambiguous large pedigree with 11 affected individuals spanning four generations is depicted in Figure 1b.

Proband 3 was a 28-year-old man who together with his wife were planning a pregnancy and was referred for genetic counseling. He had a shaved head with a big V-shaped hypopigmented patch on his forehead. Extensive areas of depigmentation on the ventral trunk and limbs could be observed with white body hair and small spots of pigmented skin. His father was similarly affected and died of hepatic cancer at 57 years of age. His mother, elder sister, and grandparents were all normal (Figure 1c).

Proband 4 was a 26-year-old man whose wife was at 16 weeks of pregnancy. The couple wanted prenatal diagnosis for the congenital leukoderma. He had a typical white forelock, V-shaped hypopigmented patch on the forehead, and large areas of leukoderma on the abdomen and limbs, with hyperpigmented spots in the affected area. His parents and other relatives were not affected (Figure 1d).

3.2 | Identification of Pathogenic Variants in the Families With Piebaldism

Four heterozygous variants in the *KIT* gene were found by WES, including c.1990+1G>A in Proband 1 (Figure 2a), c.1879+1G>A in Proband 2 (Figure 2b), c.2716T>C (p.Cys906Arg) in Proband 3 (Figure 2c), and c.1747G>A (p.Glu583Lys) in Proband 4 (Figure 2d). The c.1879+1G>A and c.2716T>C variants were paternally inherited and carried by other affected family members determined by Sanger sequencing (data not shown). The c.1990+1G>A and c.2716T>C variants were novel that could not be found in the normal population databases (1000 Genomes, EXAC, ESP6500, gnomAD, and dbSNP). They were classified as "pathogenic" (PVS1 + PM2_Supporting + PP1 + PP4) and "uncertain" (PM1 + PM2_Supporting + PP3 + PP4) according to the ACMG guidelines. The c.1747G>A and c.1879+1G>A variants have been reported previously [14, 15] and were classified as "pathogenic" with evidence of PS1 + PS2 and PVS1 + PS4 + PM2_Supporting, respectively. The PVS1 code was applied herein to the two splicing variants that were supposed to cause exon skipping and inframe translation, which might still be the loss of function. No pathogenic variants in the *SNAI2* gene were found in the four families.

3.3 | Exon Skipping Caused by the Splicing Variants

In silico tools such as ESEfinder, NNSplice, FSplice, and NetGene2 were used to predict the novel c.1990+1G>A variant, showing altered binding of splicing factors that might disrupt the original 5′ splice donor site of Intron 13 (Figure 3a). Alternative splicing was verified in vitro by a minigene reporter assay. As shown in Figure 3b, an aberrant transcription fragment (263 bp) could be

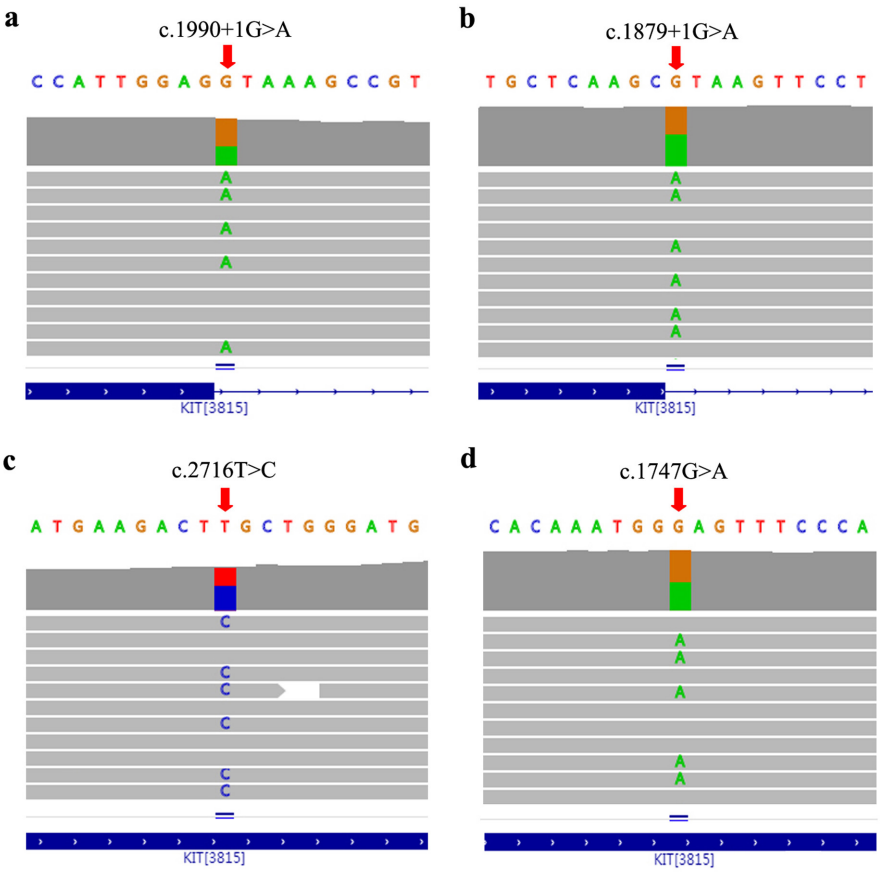

FIGURE 2 | Whole-exome sequencing revealed heterozygous variants in the *KIT* gene, including splicing variants of c.1990+1G>A in Proband 1 (a) and c.1879+1G>A in Proband 2 (b), and missense variants c.2716T>C (p.Cys906Arg) in Proband 3 (c) and c.1747G>A (p.Glu583Lys) in Proband 4 (d).

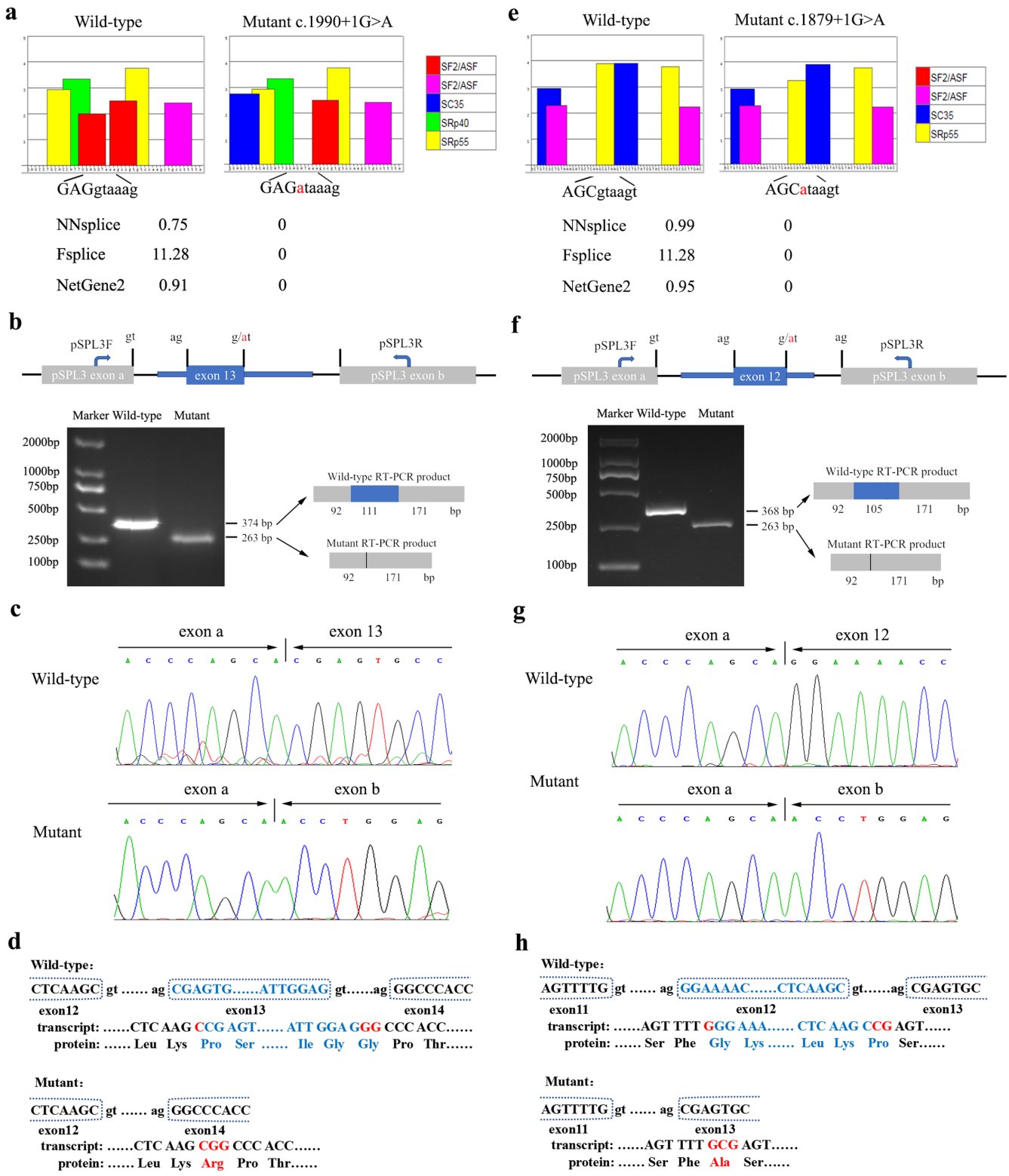

FIGURE 3 | In silico and function analyses of *KIT* splicing variants. Potential serine/arginine-rich (SR) protein binding sites were analyzed by the ESEfinder 3.0 program for c.1990+1G>A (a) and c.1879+1G>A (e) variants. ss: Splice site. The bar height represents the motif scores, and the width indicates the motif lengths along the sequence for SR proteins. Individual scores of 5′ splice sites predicated by a panel of prediction programs are shown below the charts. Transcription analysis of the c.1990+1G>A (b) and c.1879+1G>A (f) variants by minigene assay. The RT-PCR products were analyzed by agarose electrophoresis, showing smaller mutant transcripts of 263 bp compared with the wild-type constructs (374 and 368 bp). The skipping of the exon 13 by c.1990+1G>A (c) and exon 12 by c.1879+1G>A (g) was confirmed by Sanger sequencing of the purified transcripts. The truncation of proteins by c.1990+1G>A (d) and c.1879+1G>A (h) are depicted.

observed in HEK293T cells transfected with the mutant construct in contrast to that with the wild-type control (374 bp). Sanger sequencing of the RT-PCR products revealed complete skipping of Exon 13 in the c.1990+1G>A mutant transcript. The skipping would generate the substitution of Proline to Argine at Position 627, and the subsequent inframe deletion of 37 amino acids within the TK1 domain, the p.Pro627_Gly664delinsArg (Figure 3c).

The splicing variant c.1879+1G>A had been reported in two previous cases [15, 16]. Nevertheless, splicing analysis of this variant has not yet been elucidated. By in silico tools, the variant was predicted to disrupt the original 5′ splice donor site in Intron 12 (Figure 3d). The in vitro minigene reporter assay revealed an aberrant transcription fragment (263 bp) compared with the wild-type control (368 bp). The complete skipping of Exon 12 was confirmed by Sanger sequencing (Figure 3e), which accordingly could create substitution of Gly592Ala and an inframe deletion of 35 amino acids in the TK1 domain, p.Gly592_Pro627delinsAla (Figure 3f).

3.4 | Pathogenicity Analysis of the Missense Variants

The novel missense c.2716T>C variant in Exon 20 causes an amino acid substitution of p.Cys906Arg at the distal TK2 domain. Cys906 is highly conserved across various species (Figure 4a). The variant was predicted to be harmful by multiple in silico tools (data not shown). For better visualization, a 3D molecular model was constructed using the AlphaFold and PyMOL software. As shown in Figure 4b, Cys906 is located at the end of helix897-906, with its side chain in close contact with the hydrophobic residue Ile902 (4.4 Å) in the helix. The substitution of Cys906 to Arg906 changes the side chain direction and disrupts the H-bond to Ile902, which may alter the helical structural stability. Moreover, the replacement by Arg906 also creates two H-bonds to the hydrophobic residues of Tyr855 and Gly856 at the adjacent helix848-863. These conformational changes may influence the phosphorylation status of adjacent Tyr900, which is known to be important for KIT activation and subsequent signaling [17].

The missense c.1747G>A variant in exon 11 results in the amino acid change p.Glu583Lys, which locates in the N-terminal TK1 domain. Glu583 is highly conserved across various species (Figure 4a). It has been reported to be replaced by lysine, aspartic acid, and glutamine [14, 18, 19], all of which might be deleterious predicted by PolyPhen2, SIFT, REVEL, M-CAP, and MutationTaster (data not shown). As shown in the 3D molecular modeling in Figure 4c, Glu583 is located in the loop linking the JM and TK1 domains and interacts with the adjacent Tyr578 (3.2 Å) and Thr661 (2.6 Å) through H-bonds. Substitution of Glu583 to Lys583 prolongs the side chain distance to Thr661 and disrupts the H-bonds. These structural changes might influence phosphorylation status of Tyr578.

In order to evaluate the effects of the two missense variants on KIT biological function, ELISA was performed using transfected HEK293T cell lysates to determine the phosphorylation level of p-AKT and p-ERK, the two downstream signaling effectors. As shown in Figure 4d, both p-AKT and p-ERK are lower in the Cys906Arg and Glu583Lys groups than in the wild-type control, and no significant difference could be observed between the two mutant groups. These results support impaired KIT biological function by both missense variants.

3.5 | Prenatal Diagnosis and Reproductive Choice

Amniocentesis was performed for prenatal diagnosis requested by Proband 4 and his wife. Unfortunately, the fetus was confirmed to have inherited the c.1747G>A variant by Sanger sequencing. The couple finally decided to keep the fetus after in-depth post-test counselling and careful consideration and would prefer preimplantation genetic testing (PGT) for the next pregnancy. Although no genetic variants were found to be associated with the attention deficit and learning problems in the Proband 2, his parents were informed about the risk of passing down the pathogenic variant in the *KIT* gene, and they chose PGT for their second pregnancy without hesitation. Similarly, after genetic diagnosis in Probands 1 and 3, they expressed a strong desire to stop the transmission of piebaldism and preferred PGT.

3.6 | Review of Literature

Up to now, a total of 99 *KIT* variants underlying piebaldism have been reported including our case series, the majority of which were missense mutations (59.6%, 59/99). Other variants include 15 frameshift mutations, 11 splicing mutations, 5 nonsense mutations, 4 inframe insertions/deletions, 1 intragenic large deletion, as well as 3 chromosomal microdeletions covering the entire *KIT* gene and 1 chromosomal interarm inversion (inv(4)(p16q12)). As shown in Figure 5, the SNV and small indel variants have hotpots in the TK1 and TK2 domains wherein approximately 90% of the variants are associated with severe depigmentation. All the variants in the SS, EC, TM, JM, and KI domains are related to mild and moderate clinical phenotypes. As to the correlation between the phenotypic severity and variant types, the 59 missense variants are more intolerant and prone to cause severe depigmentation, with additional phenotypes including café-au-lait spots (45.8%, 27/59), brown hair (5.1%, 3/59), heterochromia irides (3.4%, 2/59), and deafness (1.7%, 1/59). However, the three patients with the entire KIT gene deletion presented mild-to-moderate phenotypes. All the cases with variants residing in the TK1 and TK2 domains in the present study had severe clinical manifestations with café-au-lait spots and no obvious intrafamilial phenotypic heterogeneity. Our data further strengthen a major pathogenic mechanism of a dominant-negative effect rather than a loss-of function in the TK domain causing severe piebaldism.

FIGURE 4 | Amino acid conservation, three-dimensional (3D) molecular modeling, and functional analyses of the *KIT* missense variants. (a) Conservative evaluation of KIT by Ugene. The Glu583 and Cys906 (indicated in a red box) are highly conserved across various species. The 3D views of the wild-type Cys906 and mutant Arg906 (b), as well as the wild-type Glu583 and mutant Lys583 (c) are built using AlphaFold and visualized by the PyMOL software. H-bonds are depicted as yellow dashed lines, and H-bond distances (Å) are indicated with black numbers. (d) Phosphorylated AKT (p-AKT) and ERK (p-ERK) levels in HEK293T cell lysates were examined by ELISA. Cells were transfected with wild-type or mutant KIT plasmids and then treated with 100 ng/mL stem cell factor (SCF) for 2 h. $^{*}p < 0.05$, and $^{**}p < 0.001$ in the ANOVA.

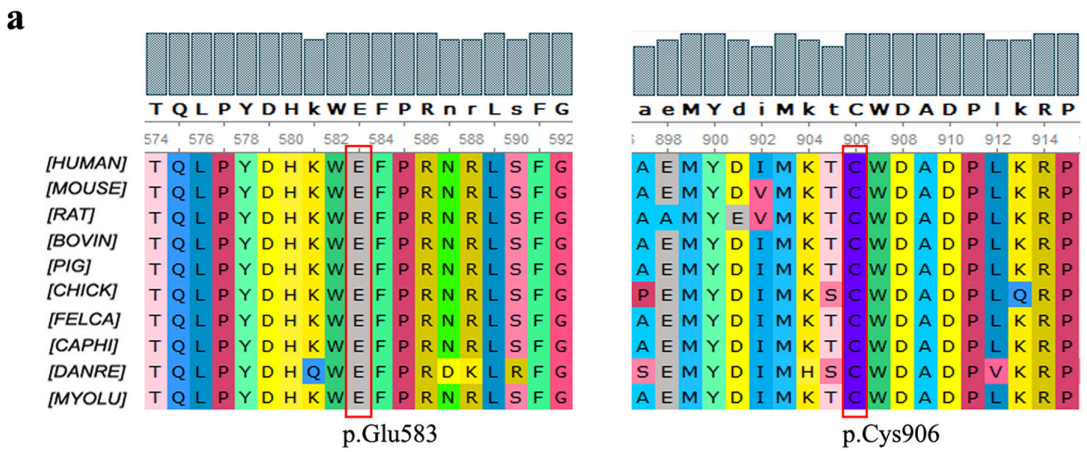
a
[HUMAN]
[MOUSE]
[RAT]
[BOVIN]
[PIG]
[CHICK]
[FELCA]
[CAPHI]
[DANRE]
[MYOLU]
p.Glu583
p.Cys906

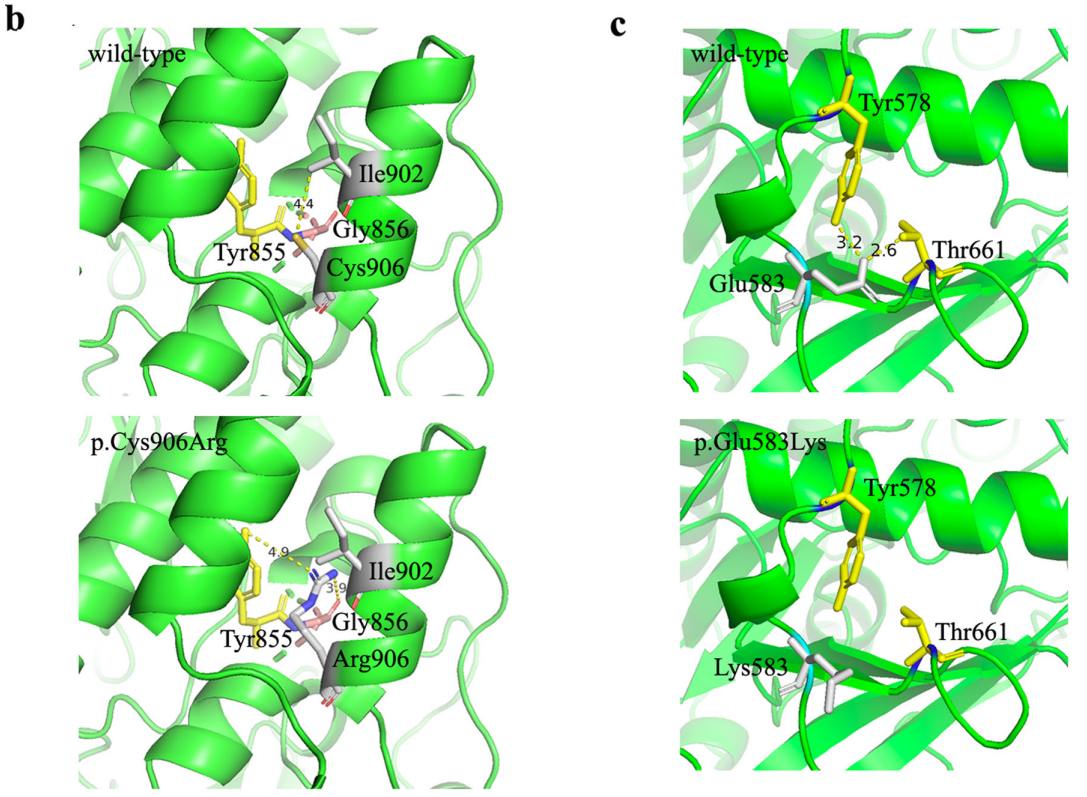
b
wild-type
Ile902
Gly856
Tyr855
Cys906
p.Cys906Arg
Arg906
c
wild-type
Tyr578
Thr661
Glu583
p.Glu583Lys
Lys583

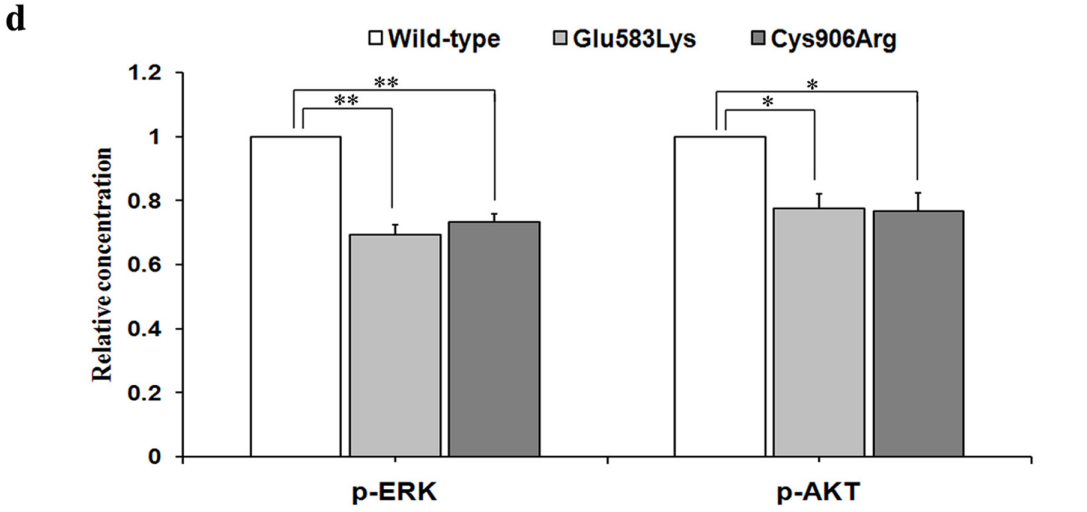
d
Wild-type
Glu583Lys
Cys906Arg
Relative concentration
p-ERK
p-AKT

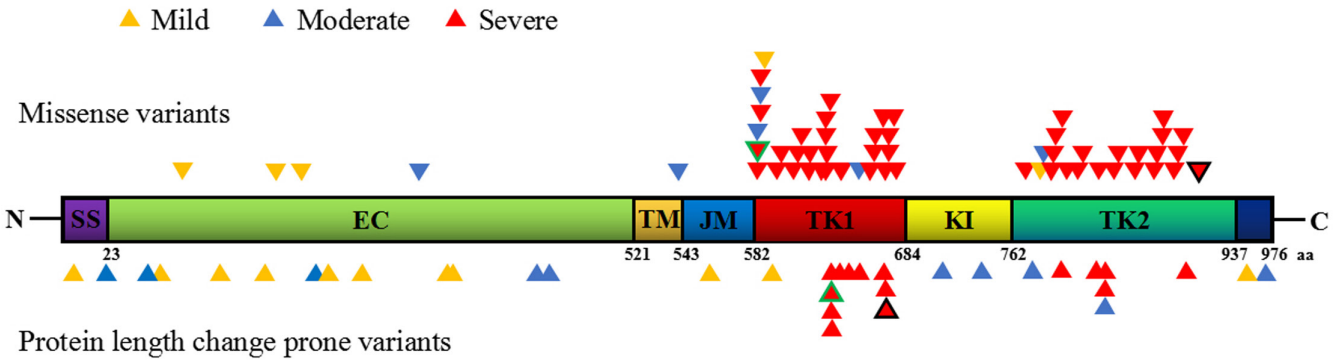

FIGURE 5 | Schematic representations of all the missense (triangles in the upper part) and protein length change prone (triangles in the lower part) variants in the *KIT* gene (NM_000222.3). The four variants identified in the present study are highlighted by framed triangles (black frames for novel variants and green frames for previously reported variants). The variants causing mild, moderate, and severe phenotypes are indicated by yellow, blue, and red, respectively.

4 | Discussion

Human piebaldism has no known racial predilection, and the prevalence of men and women is roughly equal [2]. It was first reported by Giebel and Spritz [20] and subsequently causally linked to germline mutations in the *KIT* and *SNAI2* genes. The *SNAI2* gene encodes a zinc-finger neural crest transcription factor, which is a downstream molecular target of the KIT signaling pathway and implicated in the development of human melanocytes [21]. No significant differences in the pattern, distribution, and extent of patchy hypopigmentation have been found between patients carrying variants of the two genes [12].

KIT is a Type III receptor protein-TK that triggers the phosphatidylinositol 3′ (PI3), Src family, mitogen-activated protein (MAP), and phospholipase C (PLC) kinase signaling pathways [7, 8, 22]. Somatic mutations in *KIT* are associated with leukemia, tumors of the gastrointestinal tract, and germ cells [23], whereas germline mutations in *KIT* disturb the development and migration of melanocytes and cause piebaldism. The binding of SCF to KIT leads to receptor dimerization, autophosphorylation at tyrosine residues, and the activation of protein kinase activity [24]. The key residues involved in autophosphorylation are Tyr568 and Tyr570 [25], and potentially Tyr578 in the JM domain. The c.1747G>A (p.Glu583Lys) variant in Proband 4 occurred at a highly conserved amino acid associated with Tyr578 through an H-bond, the disruption of which would influence the structural conformation and autophosphorylation of Tyr578 by 3D molecular modeling. This was supported by the observation that the homologous Glu583Lys mutation in mouse kit abolished autophosphorylation of Kit protein and caused extensive depigmentation [14]. Moreover, the phenotype of *W*37 mice was more severe than that of mice with "null" mutations, indicating a dominant-negative inhibition as the main pathogenesis. The phenotypes caused by the Glu583Asp variant is relatively less severe (extensive leukoderma but less apparent white forelock) than that caused by Glu583Lys and Glu583Gln [14, 18, 19], which may be due to the similar properties of glutamic acid and aspartic acid (both are acidic charged acids).

The TK1 and TK2 domains contain many other highly conserved enzymatic sites mediating phosphorylation and transduction of signals, among which Tyr900 in TK2 could be autophosphorylated or phosphorylated by c-Src, and subsequently interact with the p85 subunit of PI3K [17]. The activation of the PI3K cascade contributes to the regulation of melanocyte development and migration [26]. In Proband 3, the missense variant p.Cys906Arg would impair the structural conformation inside helix897-906 and disturb the biological function elicited by Tyr900 phosphorylation in the KIT kinase pathway. Moreover, the substitution by Arg906 created an interaction between helix848-863 and helix897-906 through a potential tyrosine phosphorylation site Tyr855. Functional experiment showed that both Glu583Lys and Cys906Arg variants inhibited the activation of downstream signaling molecules AKT and ERK, underlining a dominant-negative mechanism in the pathogenesis of the severe phenotype which damages over 75% of KIT functions in contrast to 50% by haploinsufficiency [27].

Some splicing variants in TKs domains could also cause severe phenotypes. The splicing variants of c.1990+1G>A and c.1879+1G>A in our study were functionally evaluated by a minigene reporter assay, showing a complete skipping of Exon 13 and Exon 12, respectively, both of which putatively causing truncated protein products with inframe deletions within the TK1 domain. Proband 1 with the c.1990+1G>A variant demonstrated severe depigmentation, similar to an 11-year-old girl from Turkey carrying the KIT c.1990+2T>G variant who had an extra phenotype of 15% hearing loss in her right ear [28]. Our patient self-reported normal hearing and denied extensive auditory examination to exclude potential hearing loss. Proband 2 with the c.1879+1G>A mutation had severe piebaldism without extracutaneous symptoms as also described in the other two cases [15, 16]. A potential pathogenic mechanism might be that heterogeneous KIT dimers with protein truncation partially lose the TK domain and therefore cannot transmit signals, leading to dominant-negative inhibition.

The presentation of leukoderma in piebaldism should be differentiated with other genodermatoses with defects in melanocyte development, such as Waardenburg syndrome (WS), Tietz syndrome, and severe PCWH syndrome (peripheral demyelinating neuropathy, central dysmyelinating leukodystrophy, WS, and Hirschsprung disease), all of which have extracutaneous

manifestations [29, 30]. Considering the common café-au-lait macules in piebaldism by reviewing the literature (45.8%, including all the four cases in the present study), the overlapping syndromes including neurofibromas I (NF1) and Legius syndrome should also be excluded [31]. Clinical diagnosis of isolated piebaldism through the typical features of congenital white forelock and depigmentation at the ventral trunk and extremities are usually unambiguous. Genetic diagnosis is still vital for the family reproductive planning. Though the disorder is stable with a benign nature, no effective therapy is available for the depigmentation which is social disabling. Reproductive choice of PGT was preferred by all the families with strong intentions to stop the disease transmission.

In conclusion, we report a case series of piebaldism caused by four germline variants in the *KIT* gene, two of which are novel. Functional experiments were carried out to elucidate the pathogenic mechanisms of the variants. The genotype–phenotype correlation was also summarized by extensive literature reviewing. Our data expanded the mutation spectrum of *KIT* and emphasized a dominant-negative effect of critical TK domains in patients with a severe phenotype. We also shared our experience in genetic counseling and prenatal diagnosis for the affected families. The limitations are in vitro evaluations of the variants using transfected cells with minigene reporter vectors and synthesized mutant expression vectors.

Author Contributions

Y.Z. involved in writing—original draft preparation. H.G. involved in methodology. X.L. involved in writing—review and editing. L.Z. involved in validation and analysis. Y.Z. contributed to resources. C.Q. contributed to conceptualization and supervision. Y.Z., X.L., and C.Q. involved in funding acquisition. All authors have read and agreed to the published version of the manuscript.

Acknowledgments

The authors are grateful to all the families for their cooperation in this study. The authors thank Professor Leping Shao at The Affiliated Qingdao Municipal Hospital of Qingdao University for kindly providing the pSPL3 vector.

Ethics Statement

The study was conducted in accordance with the Helsinki Declaration of 1964 and its later amendments and approved by the Ethics Committee of Shengjing Hospital of China Medical University (2021PS523K).

Consent

Informed consent was obtained from all subjects involved in the study. Written informed consent has been obtained from the patients to publish this paper.

Conflicts of Interest

The authors declare no conflicts of interest.

Data Availability Statement

The original contributions presented in the study are included in the article. Further inquiries can be directed to the corresponding author.

References

1. N. Oiso, K. Fukai, A. Kawada, and T. Suzuki, "Piebaldism," *The Journal of Dermatology* 40, no. 5 (2013): 330–335.

2. S. Agarwal and A. Ojha, "Piebaldism: A Brief Report and Review of the Literature," *Indian Dermatology Online Journal* 3, no. 2 (2012): 144–147.

3. L. Zhu, C. Yang, W. Zhong, et al., "KIT-Related Piebaldism in a Chinese Girl," *American Journal of Medical Genetics. Part A* 182, no. 6 (2020): 1321–1328.

4. I. Hamadah, M. Chisti, M. Haider, H. Al Dosssari, R. Alhumaidan, and B. F. Meyer, "A Novel KIT Mutation in a Family With Expanded Syndrome of Piebaldism," *JAAD Case Reports* 5, no. 7 (2019): 627–631.

5. K. Ezoe, S. A. Holmes, L. Ho, et al., "Novel Mutations and Deletions of the KIT (Steel Factor Receptor) Gene in Human Piebaldism," *American Journal of Human Genetics* 56, no. 1 (1995): 58–66.

6. S. Yuzawa, Y. Opatowsky, Z. Zhang, V. Mandiyan, I. Lax, and J. Schlessinger, "Structural Basis for Activation of the Receptor Tyrosine Kinase KIT by Stem Cell Factor," *Cell* 130, no. 2 (2007): 323–334.

7. B. Bosbach, F. Rossi, Y. Yozgat, et al., "Direct Engagement of the PI3K Pathway by Mutant KIT Dominates Oncogenic Signaling in Gastrointestinal Stromal Tumor," *Proceedings of the National Academy of Sciences of the United States of America* 114, no. 40 (2017): E8448–E8457.

8. D. Kuang, X. Zhao, G. Xiao, et al., "Stem Cell Factor/c-Kit Signaling Mediated Cardiac Stem Cell Migration via Activation of p38 MAPK," *Basic Research in Cardiology* 103, no. 3 (2008): 265–273.

9. B. Wehrle-Haller, "The Role of Kit-Ligand in Melanocyte Development and Epidermal Homeostasis," *Pigment Cell Research* 16, no. 3 (2003): 287–296.

10. K. A. Ward, C. Moss, and D. S. Sanders, "Human Piebaldism: Relationship Between Phenotype and Site of Kit Gene Mutation," *The British Journal of Dermatology* 132, no. 6 (1995): 929–935.

11. C. Wang, Y. Zhang, X. Hu, L. Wang, Z. Xu, and H. Xing, "Novel Pathogenic Variants in KIT Gene in Three Chinese Piebaldism Patients," *Frontiers in Medicine (Lausanne)* 9 (2022): 1040747.

12. M. Sánchez-Martín, J. Pérez-Losada, A. Rodríguez-García, et al., "Deletion of the SLUG (SNAI2) Gene Results in Human Piebaldism," *American Journal of Medical Genetics. Part A* 122A, no. 2 (2003): 125–132.

13. X. Liu, Y. Zhang, B. Zhang, H. Gao, and C. Qiu, "Nonsense Suppression Induced Readthrough of a Novel PAX6 Mutation in Patient-Derived Cells of Congenital Aniridia," *Molecular Genetics & Genomic Medicine* 8, no. 5 (2020): e1198.

14. R. A. Fleischman, "Human Piebald Trait Resulting From a Dominant Negative Mutant Allele of the c-Kit Membrane Receptor Gene," *The Journal of Clinical Investigation* 89, no. 6 (1992): 1713–1717.

15. R. A. Spritz, S. A. Holmes, R. Ramesar, et al., "Mutations of the KIT (Mast/Stem Cell Growth Factor Receptor) Proto-Oncogene Account for a Continuous Range of Phenotypes in Human Piebaldism," *American Journal of Human Genetics* 51, no. 5 (1992): 1058–1065.

16. K. Nagatani, K. Okamura, K. Katagiri, et al., "Report of Two Japanese Patients With Piebaldism Including a Novel Mutation in KIT," *The Journal of Dermatology* 48, no. 2 (2021): e94–e95.

17. J. Lennartsson, C. Wernstedt, U. Engström, U. Hellman, and L. Rönnstrand, "Identification of Tyr900 in the Kinase Domain of c-Kit as a Src-Dependent Phosphorylation Site Mediating Interaction With c-Crk," *Experimental Cell Research* 288, no. 1 (2003): 110–118.

18. H. Lee, S. H. Oh, K. Y. Koo, T. Suzuki, and J. S. Lee, "Novel Mutations of KIT Gene in Two Korean Patients: Variegated Shades of Phenotypes in Tyrosine Kinase 1 Domain," *Journal of Dermatological Science* 76, no. 1 (2014): 74–76.

19. M. Schabhüttl, T. Wieland, J. Senderek, et al., "Whole-Exome Sequencing in Patients With Inherited Neuropathies: Outcome and Challenges," *Journal of Neurology* 261, no. 5 (2014): 970–982.

20. L. B. Giebel and R. A. Spritz, "Mutation of the KIT (Mast/Stem Cell Growth Factor Receptor) Protooncogene in Human Piebaldism," *Proceedings of the National Academy of Sciences of the United States of America* 88, no. 19 (1991): 8696–8699.

21. J. Pérez-Losada, M. Sánchez-Martín, A. Rodríguez-García, et al., "Zinc-Finger Transcription Factor Slug Contributes to the Function of the Stem Cell Factor c-Kit Signaling Pathway," *Blood* 100, no. 4 (2002): 1274–1286.

22. R. Roskoski, Jr., "Structure and Regulation of Kit Protein-Tyrosine Kinase—The Stem Cell Factor Receptor," *Biochemical and Biophysical Research Communications* 338, no. 3 (2005): 1307–1315.

23. M. C. Heinrich, C. D. Blanke, B. J. Druker, and C. L. Corless, "Inhibition of KIT Tyrosine Kinase Activity: A Novel Molecular Approach to the Treatment of KIT-Positive Malignancies," *Journal of Clinical Oncology* 20, no. 6 (2002): 1692–1703.

24. Z. Zhang, R. Zhang, A. Joachimiak, J. Schlessinger, and X. P. Kong, "Crystal Structure of Human Stem Cell Factor: Implication for Stem Cell Factor Receptor Dimerization and Activation," *Proceedings of the National Academy of Sciences of the United States of America* 97, no. 14 (2000): 7732–7737.

25. J. Ledoux, A. Trouvé, and L. Tchertanov, "Folding and Intrinsic Disorder of the Receptor Tyrosine Kinase KIT Insert Domain Seen by Conventional Molecular Dynamics Simulations," *International Journal of Molecular Sciences* 22, no. 14 (2021): 7375.

26. J. R. Todd, L. L. Scurr, T. M. Becker, R. F. Kefford, and H. Rizos, "The MAPK Pathway Functions as a Redundant Survival Signal that Reinforces the PI3K Cascade in c-Kit Mutant Melanoma," *Oncogene* 33, no. 2 (2014): 236–245.

27. M. Hattori, O. Ishikawa, D. Oikawa, et al., "In-Frame Val216-Ser217 Deletion of KIT in Mild Piebaldism Causes Aberrant Secretion and SCF Response," *Journal of Dermatological Science* 91, no. 1 (2018): 35–42.

28. P. Syrris, K. Heathcote, R. Carrozzo, et al., "Human Piebaldism: Six Novel Mutations of the Proto-Oncogene KIT," *Human Mutation* 20, no. 3 (2002): 234.

29. M. D. Saleem, "Biology of Human Melanocyte Development, Piebaldism, and Waardenburg Syndrome," *Pediatric Dermatology* 36, no. 1 (2019): 72–84.

30. K. Inoue, K. Shilo, C. F. Boerkoel, et al., "Congenital Hypomyelinating Neuropathy, Central Dysmyelination, and Waardenburg-Hirschsprung Disease: Phenotypes Linked by SOX10 Mutation," *Annals of Neurology* 52, no. 6 (2002): 836–842.

31. C. A. Stevens, P. W. Chiang, and L. M. Messiaen, "Café-Au-Lait Macules and Intertriginous Freckling in Piebaldism: Clinical Overlap With Neurofibromatosis Type 1 and Legius Syndrome," *American Journal of Medical Genetics. Part A* 158A, no. 5 (2012): 1195–1199.